

# Spectroscopic Study Of Conformational Changes In The $\alpha$ Subunit of $F_1F_o$ ATP Synthase

Rebecca Stowe  
Chemistry  
The University of North Carolina Asheville  
One, University Heights  
Asheville, North Carolina 28804 USA

Faculty Advisor: Dr. Ryan Steed

## Abstract

$F_1F_o$  ATP synthase is present in all life and is responsible for the production of almost all adenosine triphosphate (ATP), which is one of the most prolific energy molecules that are synthesized during metabolism.  $F_o$  converts electrochemical potential into mechanical rotation, which drives conformational changes in  $F_1$  that facilitate the synthesis of ATP. The mechanism of rotation of the subunit  $c$  ring is not clear. This study looked for evidence of the ratcheting mechanism of rotation, which states that the helices of the subunit  $\alpha$ - $c$  interface act like mechanical gears during rotation. Site-directed mutagenesis was used to mutate  $\alpha$ V71C, which is located on a loop of subunit  $\alpha$ . This mutant ATP synthase was purified and then chemically modified with a spin label, which can be observed using electron paramagnetic resonance (EPR) spectroscopy. The EPR signal is sensitive to the protein environment and will provide data on the mobility of the residue to which the spin label is attached. The presence of free spin and spin dimers was too strong to allow for interpretation of the mobility of  $\alpha$ V71C. The quality of the data needs to be improved by optimization of the purification technique.

## 1. Introduction

ATP synthase is the main source of adenosine triphosphate (ATP), the universal energy currency for all living organisms.  $F_1F_o$  ATP synthase uses energy supplied by a transmembrane electrochemical gradient of  $H^+$  or  $Na^+$  to synthesize ATP.<sup>1</sup>  $H^+$  translocation down this electrochemical gradient drives a rotary mechanism of the two rotary motors  $F_1$  and  $F_o$ .  $F_1$  is a water-soluble protein complex with subunit stoichiometry  $\alpha_3\beta_3\gamma\epsilon$ .<sup>1</sup>  $F_o$  is a membrane-embedded protein complex with subunit stoichiometry  $ab_2c_{8-15}$  (Figure 1).<sup>1</sup>  $H^+$  transport occurs in the  $F_o$  sector, which drives the reaction of ATP synthesis in the  $F_1$  sector.<sup>2</sup> ATP hydrolysis can also drive the uphill movement of protons across the membrane.<sup>2</sup>

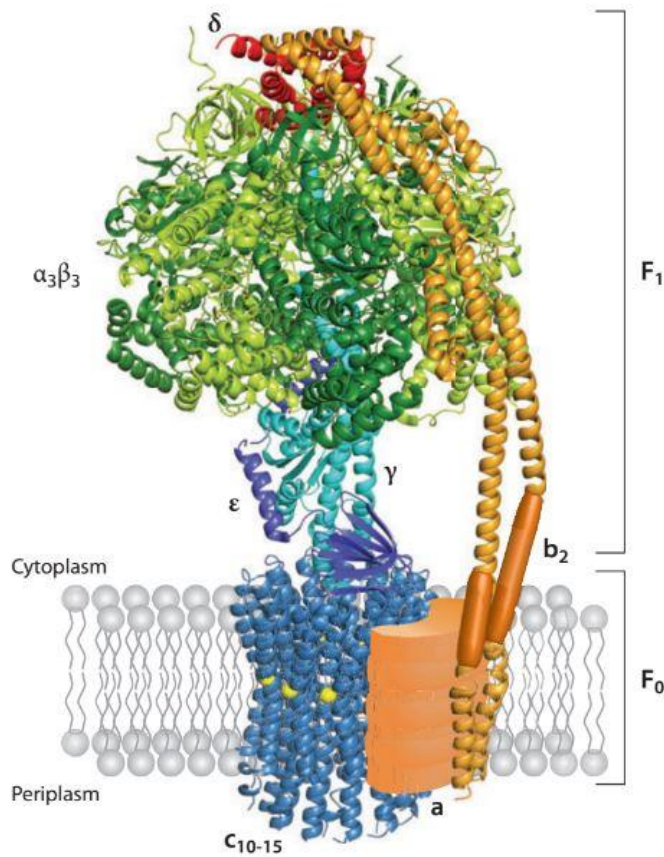


Figure 1: Structure of  $F_1F_0$  ATP Synthase with subunits labeled.<sup>1</sup>

The subunit  $a/c$  interface in the  $F_0$  motor is the site of proton translocation and therefore the site of torque generation of  $F_1F_0$  ATP synthase. A proton travels from the periplasmic side of the membrane to the middle of the membrane via one half channel located in subunit  $a$ . The  $H^+$  binds to the subunit  $c$  ring, and after the subunit  $c$  ring makes one full  $360^\circ$  rotation the  $H^+$  exits into the cytoplasm through the cytoplasmic half channel at the  $a/c$  interface. In *E. coli* ATP synthase, two residues are invariant on the subunit  $a/c$  interface, Arg210 in subunit  $a$  and Asp61 in subunit  $c$ .<sup>1</sup> Arg210 is thought to drive the release of protons from the subunit  $c$  ring binding site at Asp61.<sup>1</sup>

Structurally, few details are known about the  $F_0$  complex of ATP synthase. Some medium-resolution structures have been determined using techniques such as cryo-electron microscopy and X-ray crystallography.<sup>3</sup> A study done with X-ray crystallography on the ATP synthase of the bacterium *Paracoccus denitrificans* provided a model of interactions between subunits.<sup>3</sup> It was found that the helices of subunit  $a$  were oriented at an angle with respect to the subunit  $c$  ring.<sup>3</sup> Recent structures have shown that subunit  $a$  is tilted  $70^\circ$  off the membrane normal and that subunit  $a$  is made up of five helices with a four helix bundle.<sup>3</sup> This structure is still consistent with previous crosslinking data.<sup>3</sup> Cysteine-Cysteine (Cys-Cys) cross-linking experiments are widely used to determine interactions between subunits, such as the interactions between the helices of the subunit  $a-c$  interface.<sup>4</sup> Subunit  $b$  is flexible because the protein still functions at different lengths of subunit  $b$ .<sup>5</sup> The connections between subunits that allowed the stator subunits  $a$  and  $b$  to remain in place have yet to be resolved; higher resolution crystal structures would be needed to obtain this information.<sup>3</sup>

Cys-substitution has also been used to find areas of aqueous access within the subunit  $a/c$  interface by probing with thiolate-reactive reagents.<sup>6</sup>  $Ag^+$  was found by ATP-driven proton pumping assays, to inhibit certain Cys mutants, which lead to the conclusion that the residues that were inhibited could be aqueous accessible, and therefore part of the ion channel.<sup>6</sup> These studies provided evidence for the hypothesis that the ion channel is actually two independent ion channels separated at the proton binding site.<sup>6</sup> Additionally,  $Ag^+$ ,  $Cd^{2+}$ , and methanethiosulfonate (MTS) derivatives have been used to inhibit the mutants and determine locations of aqueous access in the  $F_0$  sector.<sup>7</sup>

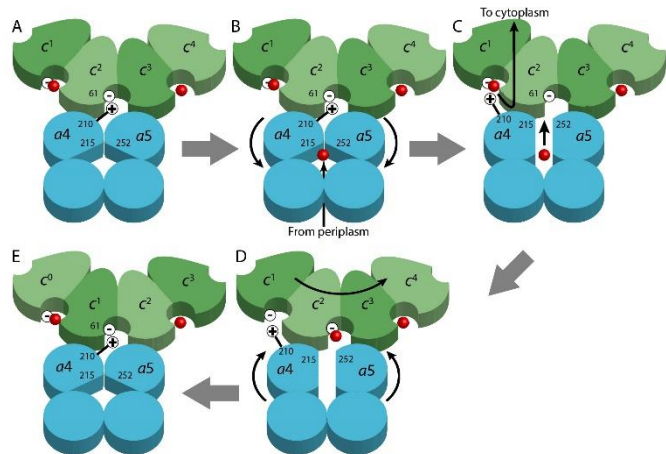


Figure 2: A diagram of the *a/c* interface showing the proposed mechanism of rotation involving proton gating by subunit *a*. The red spheres are negatively charged Asp61 residues on subunit *c*. A positive charge is shown protruding from Arg210 on subunit *a*.

The mechanism of proton translocation through  $F_0$  that generates torque and causes  $F_1$  to rotate has not been confirmed. The proposed mechanism involves the stator charge binding with each Asp61 and ejecting the protons bound at those sites, driving the rotation (Figure 2).<sup>2</sup> In order for the protons to reach the binding site on the subunit *c* ring, crosslinking evidence was found that the ion channel consists of two independent channels that are gated, and that some helices in subunit *a* may swivel.<sup>2</sup> ATP driven proton pumping was assayed in cysteine mutants and it was found that when *aTMH4-5* were crosslinked and rendered immobile, ATPase function was greatly inhibited.<sup>2,7,8</sup> This result supports a mechanical interaction in the subunit *a/c* interface, where the subunits may behave similar to gears.

Research on the mechanism of torque generation using mathematical modeling has proposed the formation of a complex between the stator charge and two Asp61 residues.<sup>9</sup> The mathematical model found that subunit *c* would drag subunit *a* with it if a single Asp61 residue was deprotonated.<sup>9</sup> In order for subunit *c* to rotate without displacing subunit *a*, two Asp61 residues would have to be deprotonated at the same time so that the stator charge formed a stable salt bridge between the desired Asp61.<sup>9</sup> This would cause the subunit *c* ring to rotate as the salt bridge was transferred between residues.<sup>9</sup> The hypothesis that subunit *b* prevented the subunit *c* ring from dragging subunit *a* along with it, has been confirmed.<sup>3</sup> The role of subunit *b* was also supported by the replacement of the N-terminus amino acid of subunit *a* with a lysine.<sup>10</sup> This replacement led to a lack of a partner residue for subunit *b*, which caused it to be displaced.<sup>10</sup>

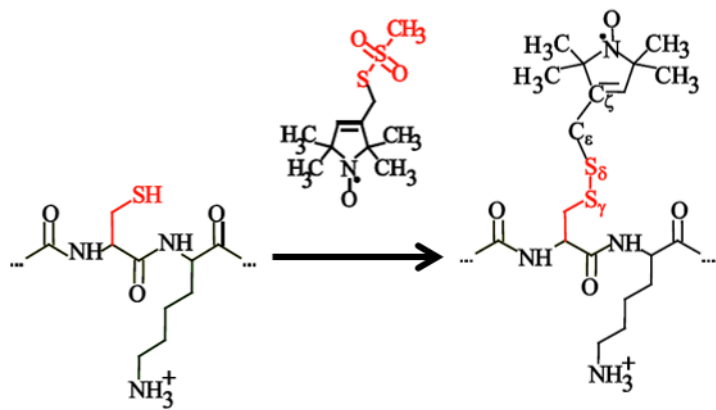


Figure 3: Spin label reaction to create the stable nitroxide radical.

A spectroscopic method known as spin labeling and electron paramagnetic resonance (EPR) has been used to observe the mobility of individual structural elements in proteins. The signals measured by EPR arise from a stable nitroxide radical attached to a Cys via an MTS. The chemical reaction of the spin label with a cysteine is shown in

Figure 3. EPR data can provide insight on mobility, solvent accessibility, polarity index of the environment, and distance between paramagnetic centers.<sup>11</sup> The environment can be manipulated in order to observe whether a residue is more exposed or more mobile under certain conditions, such as a change in pH or addition of substrate. EPR is useful for studying protein dynamics, therefore applying it to ATP synthase could determine whether the helices of subunit *a* interface are mobile when F<sub>1</sub>F<sub>0</sub> ATP synthase is functioning normally. If the residues on the interface move under normal conditions, this could provide evidence supporting a mechanical rotation mechanism.

Site-directed spin labeling and EPR has been found to be the most effective method for studying protein dynamics. Other methods such as X-ray crystallography, only show one conformation of the protein, which is only useful for solving a structure and tells nothing about mechanisms. X-ray crystallography is also extremely difficult and time consuming when used with complex proteins such as F<sub>1</sub>F<sub>0</sub>. EPR is not limited by interference or size, which gives it an advantage over other forms of spectroscopy, such as fluorescence, in the case of observing protein dynamics.<sup>12</sup> There is a possibility of EPR also giving information about structure by measuring distance between spin labels. The reliability of this technique was tested using a protein of known structure (T4L), and it was found that only 25 EPR restraints were needed to obtain a correct model.<sup>12</sup> In the case of ATP synthase, this could be used to solve the structure of subunit *a*, which has not been solved using a dynamic method.

The goal of this project is to observe conformational changes during proton translocation, and where these changes occur. In order to test for movement in subunit *a*, cysteine mutants of *E. coli* ATP synthase will be made using site directed mutagenesis, which allows for the modification of specific locations in the DNA sequence. The Cys residue will then be modified with spin labels and the mobility of the labels will be tested using EPR spectroscopy to try to determine the mobility of the residue to which the spin label is attached under various conditions. This project could provide evidence for the hypothesis of swiveling helices in subunit *a*, which will lead to a better understanding of torque generation in F<sub>1</sub>F<sub>0</sub> ATP synthase.

## 2. Experimental Methods

### 2.1 Site Directed Mutagenesis

Plasmid DNA was prepared from WT and mutant *E. coli* strains using NEB Monarch Plasmid Miniprep Kit. The DNA concentration was determined by measuring A<sub>260</sub> on a UV/Vis using a spectrophotometer. Digestion of plasmid DNA was performed with NEB BsrG1 and PflM1 restriction enzymes. The products of digestion were run on an ethidium bromide stained 1% agarose electrophoresis gel with NEB 1 kbp ladder as a standard. Ethidium bromide is a mutagen and was handled with gloves and eye protection. The DNA containing bands were extracted from the gel using an NEB DNA Gel Extraction Kit.

### 2.2 Ligation and Transformation

DNA fragments containing *a*V71C were ligated into a His-tag vector pFV2 then transformed into DH5 $\alpha$  competent cells. Cultures were grown and the plasmid DNA was purified with NEB Monarch Plasmid Miniprep Kit. Mutation was confirmed by DNA sequencing. The pure plasmid was transformed into DK8 competent cells for further experiments.

### 2.3 Preparation of inside out membrane vesicles

Three 1 L mutant cultures were grown in LB-amp medium for eight hours. The cells were centrifuged at 4000 rpm for 15 minutes to form a cell pellet. The cells were resuspended in TMG buffer (50 mM Tris, 5 mM MgCl<sub>2</sub>, 10% w/v glycerol, pH 7.5) and lysed using a cell homogenizer at 15000 psi. The lysed cells were centrifuged at 9000xg for 15 minutes to remove cell debris, then 100000xg for 30 minutes to form a membrane pellet.

### 2.4 Protein Purification

Ni-NTA resin beads were primed with wash buffer [XWL buffer (20 mM Tris, 300 mM NaCl, 100 mM sucrose, 2 mM MgCl<sub>2</sub>, 10% w/v glycerol, pH 8.0), 20 mM imidazole, 0.05% w/v dodecyl maltoside (DDM)] for affinity chromatography. The membrane pellet was equilibrated in extraction buffer (XWL buffer, 20 mM dithiothreitol, 20

mM imidazole, 1% DDM) with a glass homogenizer and rocked at 4 C for 30 minutes. The extract was then added to the primed beads and rocked for one hour at 4 C. The extraction contained 1% w/v of DDM to solubilize the membrane pellet. The extract was poured into a column and allowed to run through. Wash buffer was poured into the column to wash off any unwanted proteins. Elution buffer (XWL buffer, 200 mM imidazole, 0.05% DDM) was added to the column and 10 fractions were collected before the column was stopped. The fractions were run on a protein gel and the fractions containing protein were aliquoted to 100  $\mu$ L and stored at -80° C until use.

## 2.5 Lowry Assay

A modified Lowry Assay was performed to measure the concentration of pure  $F_1F_o$  in mg/mL.<sup>13</sup> The standards and samples were loaded into a 96 well microplate and the absorbance was read at 650 nm. The average protein concentration was measured to be 4.3 mg/mL.

## 2.6 Proton Pumping Assay

Inside out (ISO) membrane vesicles of WT and RBS071 were diluted with TMG. Thiolate specific spin label (MTSSL) in Dimethylformamide (DMF) or DMF alone were added to a sample of WT and a sample of RBS071. Fluorescence of 9-Amino-6-chloro-2-methoxyacridine (ACMA) was visualized in the fluorescence spectrometer ( $\lambda_{ex} = 415$  nm  $\lambda_{em} = 485$  nm). ATP was added to 5 mM at 20 seconds via Hamilton syringe to quench the fluorescence and nigericin was added to 0.5  $\mu$ g/mL at 100 seconds to restore fluorescence. Data acquisition was terminated at 120 seconds.

## 2.7 Spin Labeling

One shot of 20x molar excess MTSSL was added to a 4.3 mg/mL protein sample. The sample was incubated at room temperature for two hours. Another shot of MTSSL was added and the sample was incubated on ice in a fridge overnight.

## 2.8 EPR Spectroscopy

The protein sample was concentrated to 100  $\mu$ L using a spin concentrator with 100kDa cutoff. Spectra were collected at 10 mW X band microwave power with a modulation amplitude of 1.0 G and a sweep of 100 G around  $g=2$  center field. Multiple scans were averaged to reduce noise. The samples were dialyzed in buffer overnight and another spectrum was collected. To ensure the elimination of all free label, gel filtration was attempted, but the sample aggregated and was unable to be recovered. The second and third data acquisitions were performed on samples that had already been dialyzed.

## 3. Results and Discussion

Successful site directed mutagenesis of  $\alpha$ V71C was confirmed by DNA sequencing (Figure 4). Mutagenesis was performed using BsrG1 and PflM1 restriction sites to cut out a mutant region of uncB. This insert was ligated into PFV2 vector plasmid then transformed into DK8 E Coli cells, which lack a genomic copy of uncB. The mutant strain was named RBS071. Protein purification was performed on the mutant strain using Ni affinity chromatography and the fractions were run on an SDS PAGE gel. Successful purification the complete  $F_1F_o$  complex was confirmed by visualizing all nine subunits on the gel (Figure 6).

In order to prepare  $F_1F_o$  for spin labeling, cysteine must be genetically introduced into  $F_1F_o$  DNA plasmid and overexpressed in *E. coli*. Inverted vesicles must be purified from this modified strain, then the  $F_1F_o$  purified from vesicles. After purified  $\alpha$ V71C  $F_1F_o$  was confirmed to function under normal conditions, a spin label was introduced.

The function of the spin labeled protein in inverted membranes was tested using an ATP-driven proton pumping assay, and no significant difference was determined between wild type and RBS071, with or without spin label (Figure 5). This result showed that neither the mutation nor the spin label affected function of the protein. A small variation that was found in the plot of the RBS071 spin label sample was determined to be negligible and likely caused by nigericin on the tip of the needle introduced upon sample insertion. An ATPase assay was used to test the function of WT, RBS071, and RBS071 with spin label. The assays did not show any inhibition upon addition of N,N'-

dicyclohexylcarbodiimide (DCCD), which is not consistent with the presence of  $F_o$  as shown in the protein gel (Figure 6). This result suggested that the assay reagents need to be tested for possible contamination.

The purification technique was optimized by increasing the concentration of imidazole in the wash buffer from 20 mM to 30 mM to aid with the removal of undesired protein that may be attached to the His-tag. The SDS Page gel showed the presence of only one subunit in one sample, so the protein was lost at some point during the purification process.

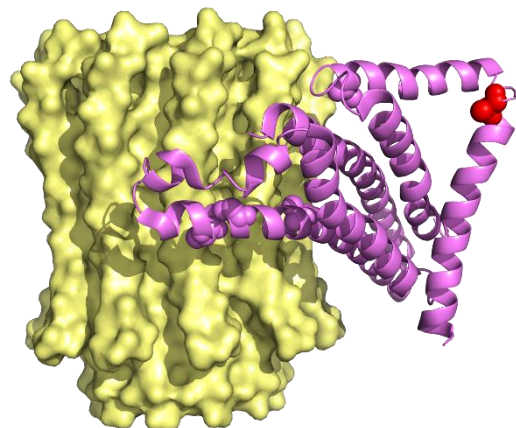


Figure 4: PyMol model of subunits *a* and *c*. Subunit *c* is shown in yellow, subunit *a* in purple, and the 071 residue is shown in red.

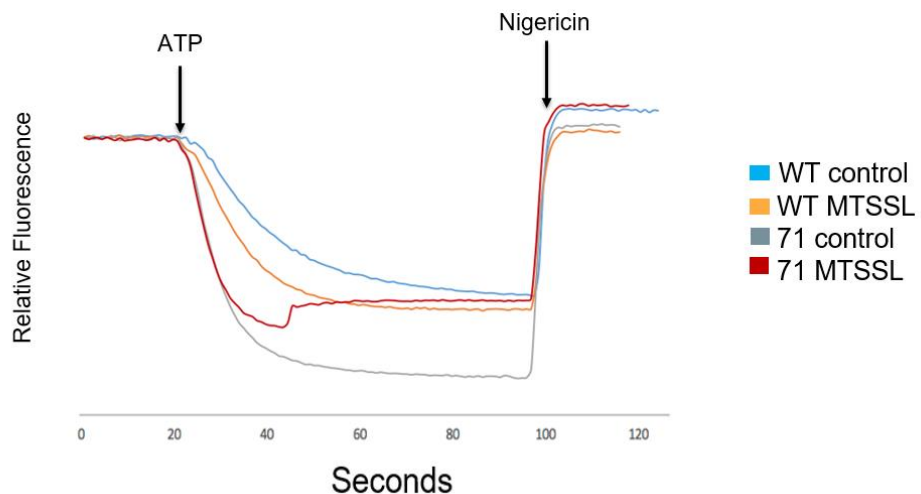


Figure 5: ATP-driven H<sup>+</sup> pumping data. The curves of the spin label samples shows no significant difference from the samples with no label.

To prepare for EPR data acquisition, the sample was spin concentrated in order to strengthen the signal. An EPR spectrum of *a*V71C F<sub>1</sub>F<sub>0</sub> with spin label was acquired (Figure 7). A spectrum was taken before and after overnight dialysis. The dialysis removed most of the free label, which cleaned up the spectrum considerably (Figure 7A). The spectral line shape indicated a level of mobility too high for spin-labeled protein, indicating the presence of free spin label. A less mobile component was visible underlying the spectrum. Two other spectra were collected at different times and both showed the presence of free spin and spin dimers (Figure 7). To get better quality data, a method must be developed to reliably remove the dimers.

A higher quality protein purification would lead to better quality data, so an optimization was attempted. After the concentration of imidazole in the wash buffer was increased from 20 mM to 30 mM the SDS page gel showed no intact protein, so 30 mM is past the upper limit. Another purification was performed at 20 mM for EPR analysis. After destaining, the gel was placed in the fridge overnight and the bands visualized more clearly than they have in past purifications. The concentration of the sample was determined to be 1.9 mg/mL by Lowry assay. This purification will be used as a reference for following optimization attempts.

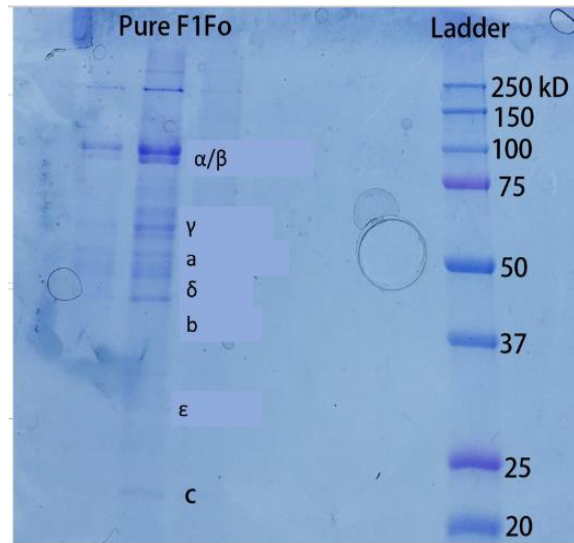
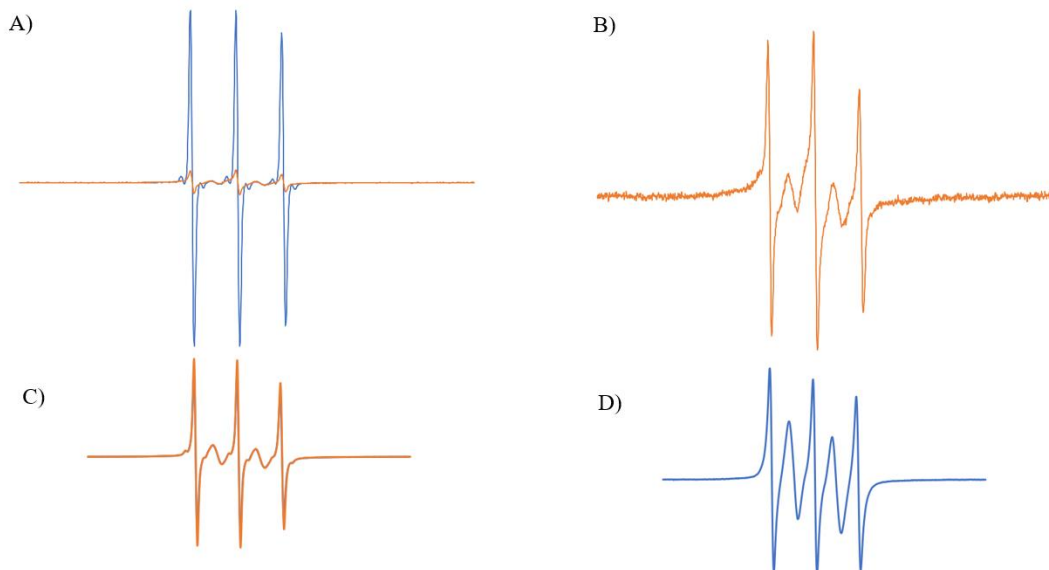


Figure 6: Protein gel containing all subunits of F<sub>1</sub>F<sub>o</sub> ATP synthase after purification.



**Figure 7:** EPR data from RBS071. Spectrum A shows both the spectra taken before (blue) and after (orange) dialysis. Spectrum B is a magnification the post-dialysis spectrum shown in spectrum A. The splitting into three lines is caused by the influence of the nuclear spin of nitrogen. Spectrum C is the second attempt at data acquisition at pH 8 (blue) and pH 5 (orange). The pH change did not visibly affect the spectrum. Spectrum D shows the third attempt of data acquisition. The presence of spin dimers in this sample made it impossible to interpret.

## 4. Conclusion

The sample quality must be improved by removal of spin dimers in order to interpret the mobility of position *a*V71C. A more efficient protein purification method must also be developed to obtain samples with higher protein concentrations and less impurities.

## 5. Acknowledgements

I would like to thank the UNC Asheville Chemistry Department, Dr. Ryan Steed, and the Steed Squad.

## 6. References

1. Von Ballmoos, Christoph; Wiedenmann, Alexander; Dimroth, Peter. Essentials for ATP Synthesis by  $F_1F_0$  ATP Synthases. *Annu. Rev. Biochem.* **2009**, *78*, 649-672.
2. Fillingame, Robert H.; Steed, P. Ryan. Half channels mediating  $H^+$  transport and the mechanism of gating in the  $F_0$  sector of *Escherichia coli* in  $F_1F_0$  ATP Synthase. *Biochim. Biophys. Acta* **2014**, *1837*, 1063-1068.
3. Morales-Rios, Edgar; Montgomery, Martin G.; Leslie, Andrew G. W.; Walker, John E. Structure of ATP Synthase from *Paracoccus denitrificans* determined by X-Ray crystallography at 4.0 Å resolution. *PNAS* **2015**, *112*, 13231-13236.
4. Jiang, Weiping; Fillingame, Robert H. Interacting helical faces of subunits *a* and *c* in the  $F_1F_0$  ATP synthase of *Escherichia coli* defined by disulfide cross-linking. *Proc. Natl. Acad. Sci USA* **1998**, *95*, 6607-6612.
5. Cain, Brian D. Mutagenic Analysis of the  $F_0$  Stator Subunits. *Journal of Bioenergetics and Biomembranes* **2000**, *32*, 365-371.
6. Schwem, Brian E.; Fillingame, Robert H. Cross-linking between Helices within Subunit *a* of *Escherichia coli* ATP Synthase Defines the Transmembrane Packing of a Four-helix Bundle. *J. Biol. Chem.* **2006**, *281*, 37861-37867.
7. Dong, Hui; Fillingame, Robert H. Chemical Reactivities of Cysteine Substitutions in Subunit *a* of ATP Synthase Define Residues Gating  $H^+$  Transport from Each Side of the Membrane. *J. Biol. Chem.* **2010**, *285*, 39811-39818.
8. Moore, Kyle J.; Fillingame, Robert H. Obstruction of Transmembrane Helical Movements in Subunit *a* Blocks Proton Pumping by  $F_1F_0$  ATP Synthase. *J. Biol. Chem.* **2013**, *288*, 25535-25541.
9. Aksimentiev, Aleksij; Balabin, Ilya A.; Fillingame, Robert H.; Schulter, Klaus. Insights into the Molecular Mechanism of Rotation in the  $F_0$  Sector of ATP Synthase. *Biophys. J.* **2004**, *86*, 1332-1344.
10. Ishmukhametov, Robert R.; DeLeon-Rangel, Jessica; Zhu, Shaotong; Vik, Steven B. Analysis of an N-terminal deletion in subunit *a* of *Escherichia coli* ATP synthase. *J. Bioenerg. Biomembr.* **2017**.
11. Hubbell, Wayne L.; Cafiso, David S.; Altenbach, Christian. Identifying conformational changes with site-directed spin labeling. *Nature Struct. Bio.* **2000**, *7*.
12. McHaourab, Hassane S.; Steed, P. Ryan; Kazmier, Kelli. Toward the Fourth Dimension of Membrane Protein Structure: Insight into Dynamics from Spin-Labeling EPR Spectroscopy. *Structure*. **2011**, *19*, 1549-1561.
13. Fillingame, R.H. *J. Bacteriol.* **1975**, *124*, 870-883.